Journal of American Science

Websites:
http://www.jofamericanscience.org
http://www.sciencepub.net

Emails:
editor@sciencepub.net
sciencepub@gmail.com

MARSLAND PRESS
Multidisciplinary Academic Journal Publisher

Exploitation of synthetized polyethylene glycol-polylactide-polyethylene glycol copolymers nanoparticles as a delivery system for intratumoral treatment of squamous cell carcinoma

Shimaa A. Elsaady[1], Essam Al-Wakeel[2], Manal F badawi[3], Moustafa N. Aboushelib[4], Sherif Refaat[5]

[1]Assistant lecturer, Department of Dental Biomaterials, Faculty of Dentistry, Zagazig University, Egypt
[2]Professor of Dental Biomaterials, Faculty of Dentistry, Mansoura University, Egypt
[3]Professor of Dental Biomaterials, Faculty of Dentistry, Mansoura University, Egypt
[4]Professor of Dental Biomaterials, Faculty of Dentistry, Alexandria University, Egypt
[5]Lecturer of medical oncology, Oncology center, Mansoura University, Egypt
Email: elsaadyshimaa710@gmail.com

Abstract: OSCC occupies more than 90% of all head and neck cancers and ranked the six most common malignant tumors worldwide. Main risk factors responsible for its occurrence were continuous exposure of alcohol, tobacco, infection of human papillomavirus and betel nut chewing. The main reason for failure to responding to available therapies was the late diagnosis of cases. **Statement of problem**: Patient difficulties on the treatment options for oral squamous cell carcinoma, which include surgery, massive dose of chemotherapy, radiotherapy, or anticancer therapy, may help eliminate unneeded side effects of the current treatment and to be the best choice of treatment which is delivery method. **Purpose:** This research article was conducted to develop and evaluate a therapeutic method of delivery intra-tumoral treatment for oral squamous cell carcinoma in mice by using polyethylene glycol-polylactide-polyethylene nanoparticles as a drug delivery system for a line of treatment consists of anticancer drug (epidermal growth factor receptor inhibitor, cetuximab) and chemotherapy (Platinol and 5FU) comparing that with the effect of delivery of a systemic treatment regarding histopathologic investigation.

[Shimaa A. Elsaady, Essam Al-Wakeel, Manal F badawi, Moustafa N. Aboushelib, Sherif Refaat . **Exploitation of synthetized polyethylene glycol-polylactide-polyethylene glycol copolymers nanoparticles as a delivery system for intratumoral treatment of squamous cell carcinoma** *J Am Sci 2021;17(11):90-98]. ISSN 1545-1003 (print); ISSN 23757264 (online). http://www.jofamericanscience.org* 2. doi: 10.7537/marsjas171121.09.

Keywords: Copolymers, Nanoparticles, Delivery system, Intratumoral treatment, Squamous cell carcinoma

1. Introduction

Squamous cell carcinoma represents a great percentage of cancers and increased in recent years.(1) It considered a challenging disease to manage in all cancer types.(2) The standard treatment for oral squamous cell carcinoma was a combination of surgery, radiation and chemotherapy. Such treatment was associated with high morbidity and function loss of the organ with 5 year survival rate. This poor prognosis was due to aggressive local invasion and metastasis and so recurrence. For that reason, new treatments, such as targeted gene therapy were being developed and being investigated in animal models. (1)

Animal models had been studied to induce squamous cell carcinomas.(1) These models permitted the identification of early diagnostic markers, understanding of the in vivo biology and genetics of tumor initiation, promotion, progression and metastasis and the development and testing of new approaches to disease prevention, novel therapeutic target and treatment.(2) To perform animal studies, a representative and reproducible tumor model in animals was needed. One of the animal models of carcinogenesis most used was that by chemical induction with 4-nitroquinoline 1-oxide.(3) It was a powerful carcinogen in several organs and it could specifically induce squamous cell carcinoma when applied in low concentrations.(4)

Drug delivery referred to approaches, formulations, technologies and systems for transporting pharmaceutical compound in the body as needed to safely achieve therapeutic effect. Nanoparticles made of poly lactice-poly ethylene glycol block-copolymer were promising vehicles for drug delivery due to their biodegradability and controllable payload release.(5) Cetuximab, Platinol and 5- fluorouracil loaded polymeric micelles were formulated using the block copolymer, poly ethylene glycol-polylactide-poly ethylene glycol, to comprehensively study their pharmaceutical application as anticancer nanomedicine.(6)

Poly ethylene glycol-polylactide-poly ethylene glycol was developed for tumor targeted drug delivery.(7) As a biocompatible water-soluble polymer, Poly ethylene glycol had widely been utilized as a hydrophilic block because of its outstanding water solubility, chain mobility, nontoxicity and non-immunogenicity. Poly lactide was a biocompatible and biodegradable polymer with low immunogenicity and favorable mechanical

properties for pharmaceutical and biomedical applications.[8] The triblock copolymer was synthesized by nanoemulsion and showed promising properties including high stability, high drug loading efficiency and successful reconstitution, compared to poly ethylene glycol-polylactide diblock copolymer.[7] In addition, poly ethylene glycol-polylactide-poly ethylene glycol showed potential as an anticancer nanomedicine for metastatic cancer by tumor-targeted drug delivery with high therapeutic efficacy.[9, 10]

2. Material and Methods

I. Lab procedures

A. Preparation and Characterization of Poly lactic Acid

PLA was synthesized through two steps, firstly, the synthesis of dicarboxylic PLA prepolymer (PLA-diCOOH), secondly, preparation of acyl halide-terminated PLA (PLA-diCOCl) prepolymer.

i. Synthesis of dicarboxylic PLA prepolymer (PLA-diCOOH)

90 wt % aqueous solution of L-lactic acid was introduced into a reactor with stannous octoate (Sn $(Oct)_2$ catalyst which was purified by vacuum distillation, and a predetermined amount of succinic acid. The mixture was stirred on a magnetic stirrer for 48 h at 180 °C for dehydration. After the mixture was cooled to room temperature, a high vacuum was applied and the temperature was gradually increased to 180 °C within 12 h. Finally the resulting product was dissolved in methylene chloride and precipitated in n-hexane followed by drying under vacuum at room temperature overnight.[11]

ii. Preparation of Acyl Halide-Terminated PLA Prepolymer (PLAdiCOCl)

All reactions were carried out in an argon-filled glass reactor which had been flame-dried prior to use. PLA-diCOOH prepolymer was dissolved in anhydrous methylene chloride and then thionyl chloride was added to the solution followed by 1 wt % of DMF. The molar ratio of PLA-diCOOH prepolymer to thionyl chloride was 1:2 and the mixture was reacted at 60°C for 4h. Finally the methylene chloride and unreacted thionyl chloride were removed under reduced pressure.[11]

B. Preparation of PEG-PLA-PEG triblock

i. Synthesis of PEG-PLA-PEG Triblock Copolymer

PLA-diCOCl prepolymer was dissolved in anhydrous methylene chloride and 1 molar ratio of PEG was introduced into the solution. The molar ratio of the PLA prepolymer to mPEG was 1:2. Anhydrous pyridine was added drop wise while the temperature was maintained at 0 °C. The reaction was carried out at room temperature for 12 h. The product mixture was precipitated into n-hexane, washed 3 successive times with hexane/methylene chloride and dried in vacuum at room temperature for 24 h. [11]

C. Micelle formation and drug loading

i. Preparation of PEG-PLA-PEG nano-micelles

The preparation method of nano-micelles was the emulsification solvent evaporation method. The process was generally divided into two steps. The first step was emulsification in which the copolymer and drugs were dissolved in organic solvent and then the emulsion was formed by adding into the water phase and stirring. The second step was to remove the organic solvent from the emulsion by evaporation. First, the copolymer was dissolved in organic solvent (acetone) and mixed with deionized water by stirring. Then, acetone was removed by evaporation and finally the micelles were obtained after freeze dehydration. [11]

ii. Preparation of PEG-PLA-PEG- Drug loaded Nanoparticles

The water-in-oil-in-water (w-o-w) solvent evaporation method was performed to fabricate the PEG-PLA-PEG- drug nanoparticles. Briefly, 10 mg of PEG-PLA-PEG was dissolved in 1 mL of trichloromethane and stirred at room temperature to obtain a uniform solution. (2 mg) of drug was dispersed in 0.2 mL of Millipore water, added to PLA solution and sonicated at 200 W for 5 min to generate the w/o primary solution. The primary solution was centrifuged at 3,000 rpm to remove free 5Fu and PLA, and emulsified with 2 mL of 2% polyvinyl alcohol solution containing Tween 80 as a surfactant by rotating at 9,500 rpm for 30 min to generate the final w/o/w emulsion. Finally, the solution was evaporated to volatile trichloromethane at 30°C for 30 min. [11]

II. Animal study

A. Animal housing:

All selected animals were housed, fed, induced, biopsed and treated in Elmowasah hospital, animal lab, Alexandria University, Egypt. A total number of healthy 20 male white mices weighting 30 gm per each and 16 weeks old age were chemically induced. They were maintained in standard polypropylene cages, at room temperature 22-25 °C, with free access to standard sterilized laboratory chow and tap water with a 12 hours light-dark cycles.

B. Carcinogenesis:

Concentrated dose of 4NQO, 70 mg/ml was applied to mices by brushing onto the hidden limb of the left leg. For each session a fresh aliquot was prepared. Pre-mechanical irritation to the area of induction prior to brushing by 4NQO resulted in better results, either by scrubbing by needle tip or by gentle brushing by H_2O_2. Anesthesia was achieved by inhalation of halothane vapour and the limb was brushed once with a no 3 camel hair brush which had been dipped in the 4NQO solution. The 4NQO induction was 16 weeks with 3times per week frequency of treatments for mice.

All mice were carefully inspected daily. After the final 4NQO application, specimen was taken from the hidden limb of each individual mouse under inhalation anesthesia 1% to 3% isoflurane (Baxter, Belgium) in 100% oxygen using an animal anesthetizing evaporator (Minerve, Esternay, France). The specimens cut and frozen at 80°C in a

solution of foetal bovin serum (50%) RPMI (40%) (Gibco) and DMSO (10%) (dimethyl sulfoxide; Sigma) to be preserved. Before the graft, specimens of tumor were defrosted for few minutes in calf foetal serum, then cut into sections of 100 mm3 and fixed in freshly made 4% buffered formalin. Subsequently, they were Haematoxylin and eosin stain (H&E) stained and microscopically examined.

C. Application of drug delivery system:

Mices were divided into 2 groups (n=10), control group recieved systemic intraperitonial injection and test group treated with intratumoral injection. On day one, 0.12 mg/ml Platinol was injected firstly, after an hour 0.06 mg/ml Cetuximab was injected. Day two to day five, 0.0144 mg/ml of 5-Fluorouracil was injected. All mices activities, movements, weights were under observation for one month. All mices were sacrificed, specimens were taken from site of tumor and histopathologically investigated.

III. Histopathological evaluation:

Specimens taken from animals must be removed carefully, without crushing, either while the animal was alive or immediately after sacrifice. Then preparation and staining the sections by (H&E) stain. Finally the sections were cleared in xylol and mounted in canada balsam to be covered with a cover slip. Be ready for histopathologic examination and routine microscopic study.

3. Results

SEM of drug loaded micelles

The particles were of spherical shape with smooth and uniform surface. They were almost similar in particle size within the same sample while there was some difference in particle size based on the variation of the preparation conditions. In both cases the average particle size for each sample was in the more or less nanoscale. Figure 1

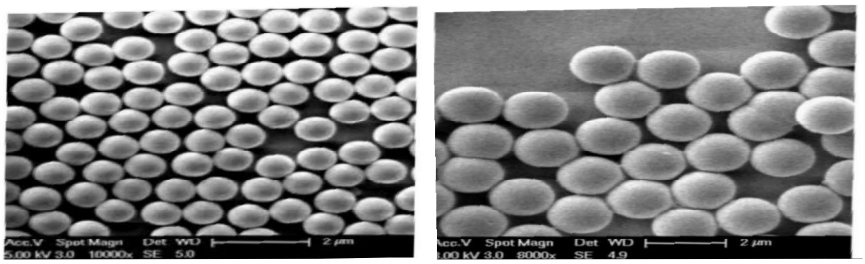

Figure 1: SEM images of the drug loaded micelles in different sizes

Drug release profile `

In vitro drug-release study from the micelles could be carried out by placing the drug loaded micelles in a suitable medium, e.g. phosphate-buffered saline (PBS) at 37 ˚C, with a stirring rate of 100 rpm and sink conditions maintained. Aliquots of the release medium were withdrawn at predetermined time intervals and the drug concentration analyzed by spectrophotometry (UV-visible spectrometer) in a 1 cm cell at 203 nm. Analysis of the data could inform the rate and cumulative amount of drug released at any given time point as shown in Figure 2,3,4 and Tables 1,2,3 for each drug loaded micelle.

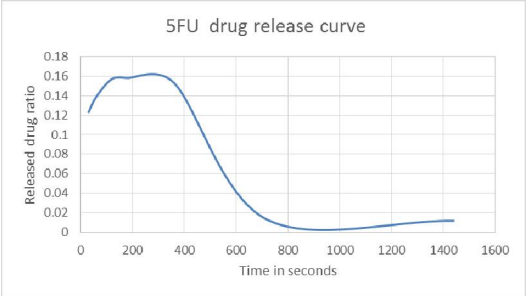

Figure 2: 5FU drug release curve

Table 1: For 5FU drug loaded micelle indicating released drug ratio at each given time.

Time of 5FU	Released ratio =II/I
5	0.154
10	0.133
15	0.138
30	0.123
60	0.139
120	0.157
180	0.158
360	0.153
720	0.013
1440	0.012

Table 2: Cisplatin drug loaded micelle indicating released drug ratio at each given time.

Time of cisplatin	Released ratio =II/I
5	0.44
10	0.438
15	0.438
30	0.435
60	0.447
2	0.446
3	0.444
6	0.44
12	0.431
24	0.436

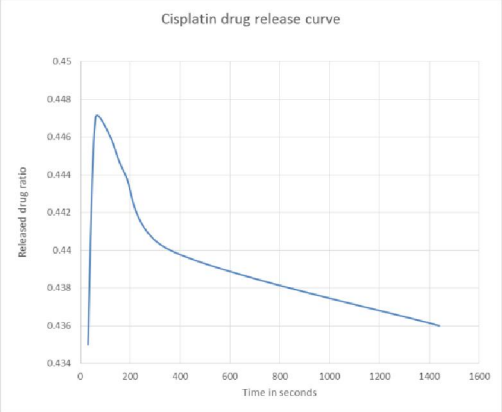

Figure 3: Cisplatin drug release curve

Table 3: For cetuximab drug loaded micelle indicating released drug ratio at each given time.

Time of Cetuximab	Released ratio
5	2.31
10	0.215
15	0.215
30	1.93
1	3.03
2	2.69
3	2.26
6	2.19
12	2.09
24	1.98

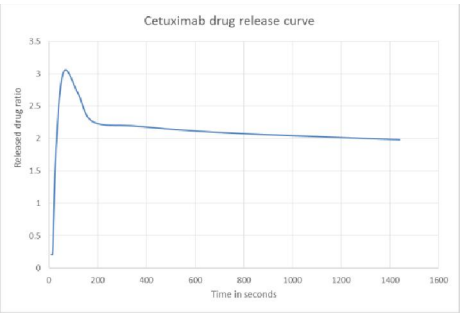

Figure 4: Cetuximab drug release curve

Histopathologic examination:

Histopathologic examination and routine microscopic study of chemically induced squamous cell carcinoma sections. These sections which were obtained from formaline-fixed-paraffin-embedded tissue blocks revealed one of these grades:

Atypia (Dysplasia):

Microscopic examination of atypia showed that it starting point was within the epidermis basal cell layer. The normal basal keratinocytes was smaller than keratinocytes and lose they lose their polarity. The appearance of the nuclei be hyperchromatic or vesicular, but comparing with the normal keratinocytes, the nuclear-cytoplasmic ratio was disrupted. As the lesions become more advanced, the normal maturation sequence was altered, with keratinocyte atypia extension was above the basal layer. Elongated rete ridges, without general thickening of the entire epidermis. As the lesions become increasing hyperplastic, there was a tendency to form downward protrusions, as rete ridges. These were a helpful feature in the diagnosis of some cases it was markedly increased over the normal frequency of the rete ridge pattern. The pathognomonic feature was the keratinocytes cytologic atypia. **Figure 5**

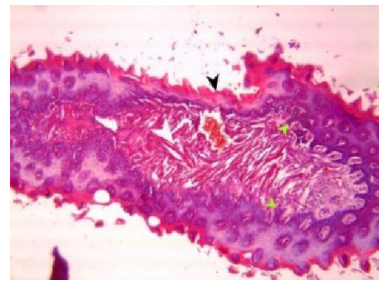

(a)

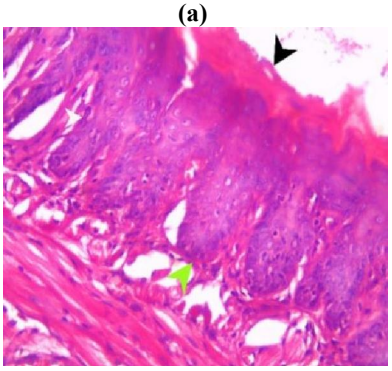

(b)

Figure 5 a, b: Images of histopathologic examination of specimen of mild and moderate atypia (dysplasia)

Squamous carcinoma insitu:

Microscopic examination revealed a stratified squamous epithelial lining showing a marked dysplastic changes involving all layers of epithelial lining forming carcinoma insitu. The dysplastic cells were made up of pleomorphic cells, having abundant deep eosinophilic cytoplasm and pleomorphic nuclei having prominent nucleoli and atypical mitotic figures. There was foci of microinvasion showing small nests of malignant cells embedded in the subepithelial layer. **Figure 6**

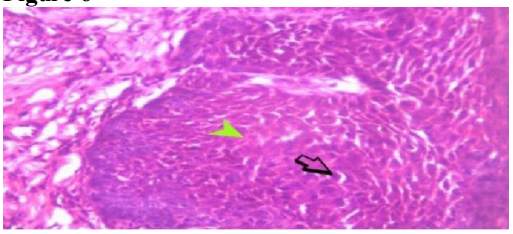

Figure 6: Image of histopathologic examination of specimen of carci-noma insitu (high power of elongated rete ridges)

Squamous cell carcinoma grade 1 (well differentiated Squamous cell carcinoma):

Microscopic examination revealed partially-ulcerated stratified squamous epithelial lining infiltrated by a neoplastic growth made up of nests of malignant epidermoid cells having central keratin pearls. The neoplastic cells have abundant deep eosinophilic cytoplasm and pleomorphic hyperchromatic nuclei having prominent nucleoli. Few atypical mitotic figures were noted. The neoplastic nests were separated by fibroblastic stroma entangling inflammatory cells. **Figure 7**

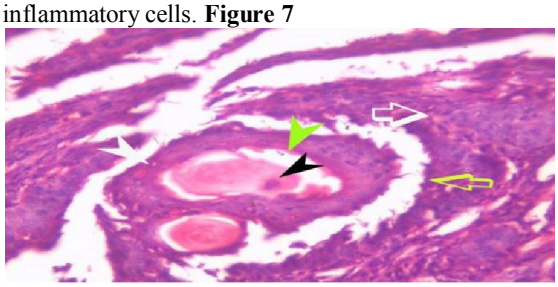

Figure 7: Image of histopathologic examination of specimen of squamous cell carcinoma grade 1(high power)

S**quamous cell carcinoma grade 2 (moderate differentiated Squamous cell carcinoma**):

Microscopic examination of tissue fragments reveal neoplastic growth formed of diffuse sheets, nests and trabecular structures of large pleomorphic malignant epidermoid cells separated by scanty stroma. The neoplastic cells have large pleomorphic hyperchromatic nuclei with prominent nucleoli. Moderate atypical mitotic figures as well as foci of intracellular keratinization and few keratin pearls were seen. **Figure 8**

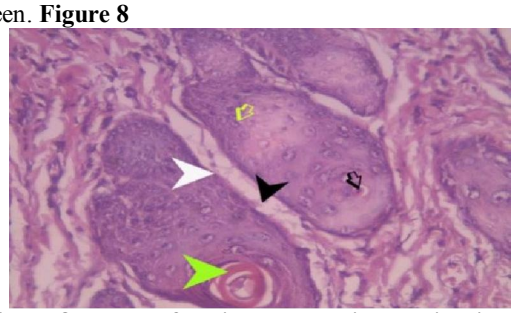

Figure 8: Images for histopathologic examination of specimen of squamous cell carcinoma grade 2 (high power)

0.Squamous cell carcinoma grade 3 (poorly differentiated Squamous cell carcinoma):

Tissue fragments reveal neoplastic growth formed of diffuse sheets, nests and trabecular structures of large pleomorphic malignant epidermoid cells separated by scanty stroma. The neoplastic cells have large pleomorphic hyperchromatic nuclei with prominent nucleoli. Frequent atypical mitotic figures as well as foci of intracellular keratinization were seen. **Figure 9**

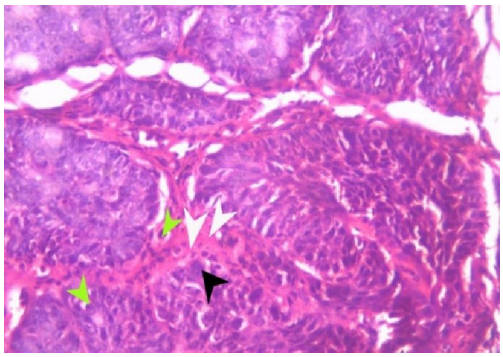

Figure 9: Image of histopathologic examination of specimen of squamous cell carcinoma grade 3 (high power)

Histopathologic examination and routine microscopic study of total oral chemically induced squamous cell carcinoma sections after application of treatment either intraperitonial or intratumoral injection. These sections which were obtained from formaline-fixed-paraffin-embedded tissue blocks revealed one of the following observstions:

i. Normal healthy tissue Figure 10

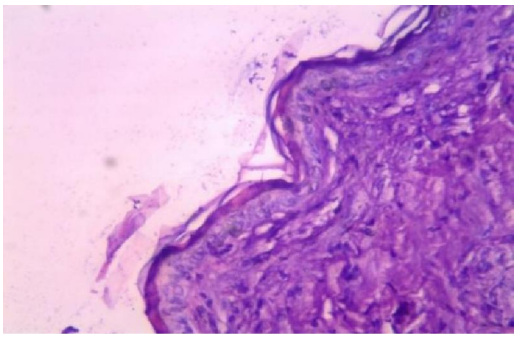

ii. Necrosis:

Necrosis occurred in epidermis cells as sheets of neutrophils (inflammatory cells) and goast tumor cells in which it was difficult to differentiate between all components of cells either nucleus or cytoplasm or any other components. **Figure 11**

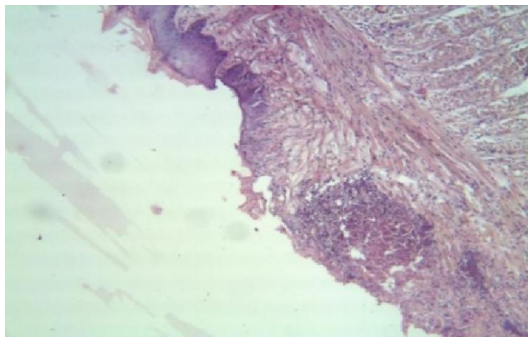

4. Discussion:

The present study was seeking for novel and current pharmaceutical approaches for management

of OSCC, outlines treatments and formulation approaches such as targeted site-specific nanotechnology-based formulation for the effective treatment of OSCC with excluding the hazardous effect of systemic treatment, so we tried to upload an effective 1st-line regimen of platinum, 5-fluorouracil and cetuximab with its great advantageous intratumoral based on a nanotechnology formulation to address unmet needs for the treatment of oral cancer.

I. Preparation, characterization of triblock copolymer and drug selection

New drug delivery approaches in oral cancer focused on intra-tumoral or local drug delivery.[11] There was a remarkable progress in over the last 20 years in biomedical applications of smart-block based nanomicelles development and achievement. These injectable nanomicelles had many advantages as non-invasive administration, cytocompatibility, tunable mechanical properties, highly permeability, controllable degradability, injectability and ability to deliver bioactive molecules and/or cells for a variety of biomedical applications. Based on these advantageous and the development of smart-block for fabrication of injectable nano-micelles and their potential biomedical applications it was selected to be our study basis.[12] Their capability of increasing the solubility and stability of hydrophobic drugs and in vivo therapeutic efficacy that was comparable or superior to the free drug.[13]

Cagel M,[14] discussed the scheme of micelle formation and stability. The two forces that were responsible for the micelle formation were attractive and repulsive forces, whereby the attractive forces resulted in the association of polymer molecules and the repulsive forces inhibited the unrestricted growth of the micelles into the macroscopic stage. At lesser concentrations, the polymers function as single chains but with the increase in the concentrations to CMC, the polymers started assembling in a way that the hydrophobic component was away from the aqueous part. Above the CMC, the co-polymers continued to self-assemble to form stable micelles where the inner core was hydrophobic and the outer corona was the hydrophilic part and the micelle formation was complete when the structure arrived at its lowest free energy configuration.

With the agreement of current study, PLA based polymers had been extensively studied in literature, thanks to their interesting properties for the synthesis of nanoparticles for drug delivery. Nanoparticles showed a great potential as nano-carriers to deliver poorly soluble drugs, targeting the tumor and releasing the active compound at the desired rate, enhancing in the therapeutic effect. These materials had demonstrated superiority compared to non-degradable counterparts and hold great translational potential in various clinical settings.[15]

In agreement with current study results, in 2020, Nairrita concluded that PEG was the polymer of choice and was approved by the FDA for clinical application, mostly because of its molecular weight (1–15 kDa) and biocompatibility that provided an optimum residence time in the body. Longer PEG chains resulted in increased circulation time in vivo, due to the resultant denser hydrophilic shell. The hydrophilic shell could also be made up of PEG that provided stealth properties to the micelle and lead to efficient bio-distribution by bypassing the MPS uptake.[16]

Unlike the present study, another effort suggested that these systems suffered from problems such as instability of protein drugs during synthesis of nanoparticles or release process due to protein contact with organic hydrophobic phase and production of acidic environment as the result of polymer degradation. [17]

With respect to PLA and PEG advantageous and to resolve the problems of systemic intravenous injection of targeted anticancer drug and chemotherapy especially for such debilitated cancerous patients, PEG-PLA-PEG polymeric systems had been selected in the current study for the purpose of targeted, intra-tumoral, gradual and sustained release of anticancer drugs and hence reducing the need for systemic intravenous injections and their drawbacks.

one study that assured our current study results in usage of cisplatin loaded nanoparticles for tumor growth suppression in mice with OSCC was done by Carson et al.[18] Another study assured our current study results in usage of cisplatin loaded nanoparticles for tumor growth suppression in mice with OSCC was done by Carson et al.[19] Coupling of drugs together which was applied in the present study was in agreement with Kerr, W.G[20] results in 2019, discovered a novel immunotherapy strategy involved using small molecules as monotherapy or combined with other anticancer therapies. The main advantages of these small molecules were good oral bioavailability, ability to penetrate the physiological barriers, precise formulations and dosing options and lower cost to produce and administer.

With agreement of current study findings, there were more recent data showing a survival benefit for patients with recurrent/metastatic disease who were treated with a 1st-line regimen of platinum, fluorouracil and cetuximab. These promising results had a significant impact on the standard of care for HNSCC, allow to decrease the morbidity of treatment and had prompted further research on the role of EGFR inhibitors in the treatment of HNSCC.[21, 22] In 2008, Ranee Mehra, M.D[23] concluded that Cetuximab was an active drug in head and neck cancer, with evidence that when given with radiotherapy or cisplatin chemotherapy resulted in better response. Its favorable toxicity profile in combination with radiation offered an advance in the standard management of patients with locally advanced disease who were not

good candidates for cisplatin. At this time lack of biomarkers to define those patients most likely to respond (or not respond) to EGFR-based therapies. Further study of the best way to integrate cetuximab, in conjunction with newer agents, into practice improved the effectiveness of treatment for HNSCC.

Characterization:

Characterization of the micellar structure determined the structural integrity of the polymers used to design the polymeric micelle formulation, the morphology of nanoparticles and drug release profile.

Morphological evaluation

TEM was used to directly observe the structures of nanoparticles and to examine the micelle morphology and particle size. The TEM images of the present study suggested that nanoparticles were irregularly shaped and were constructed from small copolymer clusters. With around average diameter 30-300 nm in size. It also could be reasonable to assume that nanoparticles had a better drug/ copolymer-packed structure. According to the results of SEM of synthetized nanoparticles, it was shown that nanoparticles of the triblock copolymer had regular spherical structure with smooth and uniform surfaces without signs of collapse, which was a good sign for an enhanced encapsulation efficiency and a more consistent structure.

In vitro drug-release study

Some studies improved the solubility of hydrophobic drugs was improved by adding Tween 80, making the invitro drug release study of hydrophobic drugs encapsulated in polymeric micelles both easier and a closer approximation of invivo conditions but in our current study there was no need for such way of stability as the drug-loaded micelles used in the present study were stable enough.[24]

Cetuximab, Cisplatin and 5FU release from nanoparticles was measured under constant physiological conditions (pH 7.4 and temperature of 37 °C). It had been expressed that drug release of nanoparticles synthesized by W/O/W method had an initial burst release followed by a multi-step slow release. Initial burst release occurred in the first hours of drug release process which was related to proteins located on the surface or near the surface of nanoparticles in the channels establishing the linkage between the internal droplets and external aqueous phase formed during organic solvent removal process and hardened at the stage of nanomicelles solidification. The extent of this release depend on composition of polymer and some other factors.[25]

In the second phase of drug release, encapsulated proteins would be released through both diffusion and gradual degradation of PEG matrix due to hydrolysis in water. For sustained release system, a small initial burst release and a constant drug release phase were desirable. The drug release profile of three diferent triblock copolymeric nanosmicelles was different. The reason for such difference in drug release profile could be found in different hydrolysis-induced degradation rate of polymers. So that enhancing the ratio of hydrophilic PEG to hydrophobic sequence of PLA had increased the water diffusion to the system and subsequently polymer destruction and drug release increased. But another issue was incomplete release of drug from these drug-carrying nanosystems whose one of the reasons was non-specific adsorption of protein to PLA blocks. One study had reported that some proteins were entrapped in hydrophobic matrix of drug delivery systems like PLA sections and provide incomplete release of drug due to non-specific adsorption of drug.[26]

II. Squamous cell carcinoma and induction of tumor

Experimental animal models that accurately represent the cellular and molecular changes associated with the initiation and progression of human cancer, were of crucial importance, although some were more suited for certain applications than others.[27] In agreement with the current study, Frese KK,[28] indicated that mice were one of the best model organisms for cancer research because of the animals' small size, propensity to breed in captivity, life span of 2-3 years, many physiological and molecular similarities to humans and fully sequenced genome in mouse models of OSCC, xenograft models and chemical carcinogen-induced models were widely used.

Unlike our present study, Szaniszlo P[29] decided to choose xenograft models with implanted human OSCC cells to study human tumor growth and spread as well as to develop and test new antitumor drugs. Animal models of chemical carcinogenesis, compared with transplantation models, might more accurately reflect the clinical course of human disease.[30] Advantages were the speed and certainty of tumor development. The premier limitation was the lack of functional T lymphocytes in these type of mice resulting in a non physiological tumor response.

In agreement with the current study, Wilkey et al., 2009[31] reported that 4NQO was a synthetic carcinogen derivative of a quinoline, soluble in water, sensitive to high temperature and light was used to study the various stages of oral carcinogenesis, because it was capable of inducing sequentially the phases of carcinogenesis (dysplasia, severe dysplasia, carcinoma in situ and OSSC with its different grades).

In the current study, it was also found that 4-6 months brushing with No. 3 camel brush on the hidden part of the left leg of the mice with prior mechanical irritation by needle tip rubbing or H2O2 with ascending doses of 4NQO resulted in typical OSCC lesions. Pathological analysis indicated that these lesions and tumors were flat squamous dysplasias (from mild to severe atypia), carcinoma in situ (non-invasive SCC) and invasive SCC (well, modertaly and poorly differentiated SCC).[32] Multiple lesions were considered to constitute the multi-step carcinogenesis of OSCC; this multi-step process was one advantage of the 4NQO model and

the development of fully malignant SCC was preceded by increasing grades of dysplastic changes that mimic cancer development in humans.[33] Contrary to our study, SCCs take long time to be detected. They were typically detected between 12 and 33 weeks after applying 4NQO (via drinking water) [34, 35] which assured that brushing on the leg give fast, confirmed and better results than application in drinking water.

Conclusion:

Based on the results, the following conclusions could be made:

Mices treated with intra-tumoral injection of drug-loaded nanomicelles gave better responses and results than those treated with intra-peritoneal injection by 100% curing which also confirmed histopathologically.

PEG-PLA-PEG block copolymers, with their biodegradability, good biocompatibility and amphiphilic they could be used as many nanoparticles. By changing the PEG-PLA ratio and the Mw and content of PLA and PEG, the block copolymers could elevate the hydrophobic drug loading and encapsulation efficiency, particle sizes reduction, increase time of blood circulation and avoid the reticuloendothelial system recognition.

References

(1). **Martínez CAR.** 4NQO carcinogenesis: A model of oral squamous cell carcinoma. International Journal of Morphology. 2012; 30(1): 309-14.

(2). **Boffetta P, Hashibe M.** Alcohol and cancer. The Lancet Oncology. 2006; 7(2): 149-56.

(3). **El-Rouby DH.** Histological and immunohistochemical evaluation of the chemopreventive role of lycopene in tongue carcinogenesis induced by 4-nitroquinoline-1-oxide. Archives of Oral Biology. 2011; 56(7): 664-71.

(4). **Guijarro-Martínez R, Gellrich NC, Witte J, Tapioles D, von Briel C, Kolotas C, et al.** Optimization of the interface between radiology, surgery, radiotherapy, and pathology in head and neck tumor surgery: a navigation-assisted multidisciplinary network. International Journal of Oral and Maxillofacial Surgery. 2014; 43(2): 156-62.

(5). **Kumar V, Abbas AK, Fausto N.** Patología estructural y funcional: Robbins y Cotran: Harcourt Brace De Espana Sa; 2005.

(6). **Nampoothiri KM, Nair NR, John RP.** An overview of the recent developments in polylactide (PLA) research. Bioresource technology. 2010; 101(22): 8493-501.

(7). **Schoop RAL, Noteborn MHM, Baatenburg de Jong RJ.** A mouse model for oral squamous cell carcinoma. Journal of Molecular Histology. 2009; 40(3): 177-81.

(8). **Song H-T, Hoang NH, Yun JM, Park YJ, Song EH, Lee ES, et al.** Development of a new tri-block copolymer with a functional end and its feasibility for treatment of metastatic breast cancer. Colloids and Surfaces B: Biointerfaces. 2016; 144: 73-80.

(9). **Videtic GM, Stitt LW, Dar AR, Kocha WI, Tomiak AT, Truong PT, et al.** Continued cigarette smoking by patients receiving concurrent chemoradiotherapy for limited-stage small-cell lung cancer is associated with decreased survival. Journal of Clinical Oncology. 2003; 21(8): 1544-9.

(10). **Shalgunov V, Zaytseva-Zotova D, Zintchenko A, Levada T, Shilov Y, Andreyev D, et al.** Comprehensive study of the drug delivery properties of poly(l -lactide)-poly(ethylene glycol) nanoparticles in rats and tumor-bearing mice. Journal of Controlled Release. 2017; 261: 31-42.

(11). **Hesong Zhao, Zhun Liu, Sanghyuk Park, Sang-Ho Kim, Jung-Hyun Kim and Longhai Piao.** Preparation and Characterization of PEG/PLA Multiblock and Triblock Copolymer. Bull. Korean Chem. Soc. 2012; 33(5): 1638:42.

(12). **Ketabat, Pundir, Mohabatpour, Lobanova, Koutsopoulos, Hadjiiski, et al.** Controlled Drug Delivery Systems for Oral Cancer Treatment-Current Status and Future Perspectives. Pharmaceutics. 2019; 11(7): 302.

(13). **Hoang Thi TT, Sinh LH, Huynh DP, Nguyen DH, Huynh C.** Self-assemblable polymer smart-blocks for temperature-induced injectable hydrogel in biomedical applications. Frontiers in chemistry. 2020; 8: 19.

(14). **Cagel M, Tesan FC, Bernabeu E, Salgueiro MJ, Zubillaga MB, Moretton MA, et al.** Polymeric mixed micelles as nanomedicines: Achievements and perspectives. European Journal of Pharmaceutics and Biopharmaceutics. 2017; 113: 211-28.

(15). **Movassaghian S, Merkel OM, Torchilin VP.** Applications of polymer micelles for imaging and drug delivery. Wiley Interdisciplinary Reviews: Nanomedicine and Nanobiotechnology. 2015; 7(5): 691-707.

(16). **Majumder N, G Das N, Das SK.** Polymeric micelles for anticancer drug delivery. Therapeutic Delivery. 2020; 11(10): 613-35.

(17). **Ghaz-Jahanian MA, Abbaspour-Aghdam F, Anarjan N, Berenjian A, Jafarizadeh-Malmiri H**. Application of chitosan-based nanocarriers in tumor-targeted drug delivery. Molecular biotechnology. 2015; 57(3): 201-18.

(18). **Ye C, Chi H**. A review of recent progress in drug and protein encapsulation: Approaches, applications and challenges. Materials Science and Engineering: C. 2018; 83: 233-46.

(19). **Carson AR, McTiernan CF, Lavery L, Grata M, Leng X, Wang J, et al.** Ultrasound-Targeted

Microbubble Destruction to Deliver siRNA Cancer Therapy. Cancer Research. 2012; 72(23): 6191-9.

(20). **Kerr WG, Chisholm JD.** The next generation of immunotherapy for cancer: small molecules could make big waves. The Journal of Immunology. 2019; 202(1): 11-9.

(21)11. **Zhao H, Liu Z, Park S-H, Kim S-H, Kim J-H, Piao L.** Preparation and Characterization of PEG/PLA Multiblock and Triblock Copolymer. Bulletin of the Korean Chemical Society. 2012; 33(5): 638-42.

(22). **Guigay J, Tahara M, Licitra L, Keilholz U, Friesland S, Witzler P, et al.** The evolving role of taxanes in combination with cetuximab for the treatment of recurrent and/or metastatic squamous cell carcinoma of the head and neck: evidence, advantages, and future directions. Frontiers in oncology. 2019; 9: 66-8.

(23). **Mehra R, Cohen RB, Burtness BA**. The role of cetuximab for the treatment of squamous cell carcinoma of the head and neck. Clinical advances in hematology & oncology: H&O. 2008; 6(10): 7-42.

(24). **Koshani R, Jafari SM.** Nuclear magnetic resonance (NMR) spectroscopy of nanoencapsulated food ingredients. Characterization of Nanoencapsulated Food Ingredients: Elsevier; 2020; 411-58.

(25). **Mallery S, Desai K-G, Holpuch A, Schwendeman S.** Optimizing therapeutic efficacy of chemopreventive agents: A critical review of delivery strategies in oral cancer chemoprevention clinical trials. Journal of Carcinogenesis. 2011; 10(1): 23.

(26). **Mallery SR, Tong M, Shumway BS, Curran AE, Larsen PE, Ness GM, et al.** Topical Application of a Mucoadhesive Freeze-Dried Black Raspberry Gel Induces Clinical and Histologic Regression and Reduces Loss of Heterozygosity Events in Premalignant Oral Intraepithelial Lesions: Results from a Multicentered, Placebo-Controlled Clinical Trial. Clinical Cancer Research. 2014; 20(7): 1910-24.

(27). **Puts MTE, Tu HA, Tourangeau A, Howell D, Fitch M, Springall E, et al.** Factors influencing adherence to cancer treatment in older adults with cancer: a systematic review. Annals of Oncology. 2014; 25(3): 564-77.

(28). **Frese KK, Tuveson DA.** Maximizing mouse cancer models. Nature Reviews Cancer. 2007; 7(9): 654-8.

(29). **Szaniszlo P, Fennewald SM, Qiu S, Kantara C, Shilagard T, Vargas G, et al.** Temporal characterization of lymphatic metastasis in an orthotopic mouse model of oral cancer. Head & neck. 2014; 36(11): 638-47.

(30). **Gimenez‐Conti IB, Slaga TJ.** The hamster cheek pouch carcinogenesis model. Journal of Cellular Biochemistry. 1993; 53(S17F): 83-90.

(31). **Wilkey JF, Buchberger G, Saucier K, Patel SM, Eisenberg E, Nakagawa H, et al.** Cyclin D1 overexpression increases susceptibility to 4-nitroquinoline-1-oxide-induced dysplasia and neoplasia in murine squamous oral epithelium. Molecular Carcinogenesis. 2009; 48(9): 853-61.

(32). **Deuerling L, Gaida K, Neumann H, Remmerbach TW.** Evaluation of the accuracy of liquid-based oral brush cytology in screening for oral squamous cell carcinoma. Cancers. 2019; 11(11): 181-3.

(33). **Ranganathan K, Kavitha L**. Oral epithelial dysplasia: Classifications and clinical relevance in risk assessment of oral potentially malignant disorders. Journal of oral and maxillofacial pathology: JOMFP. 2019; 23(1): 19.

(34). **Tang XH.** Oral Cavity and Esophageal Carcinogenesis Modeled in Carcinogen-Treated Mice. Clinical Cancer Research. 2004; 10(1): 301-13.

(35). **Hawkins BL, Heniford BW, Ackermann DM, Leonberger M, Martinez SA, Hendler FJ.** 4NQO carcinogenesis: A mouse model of oral cavity squamous cell carcinoma. Head & Neck. 1994; 16(5): 424-32.

11/12/2021